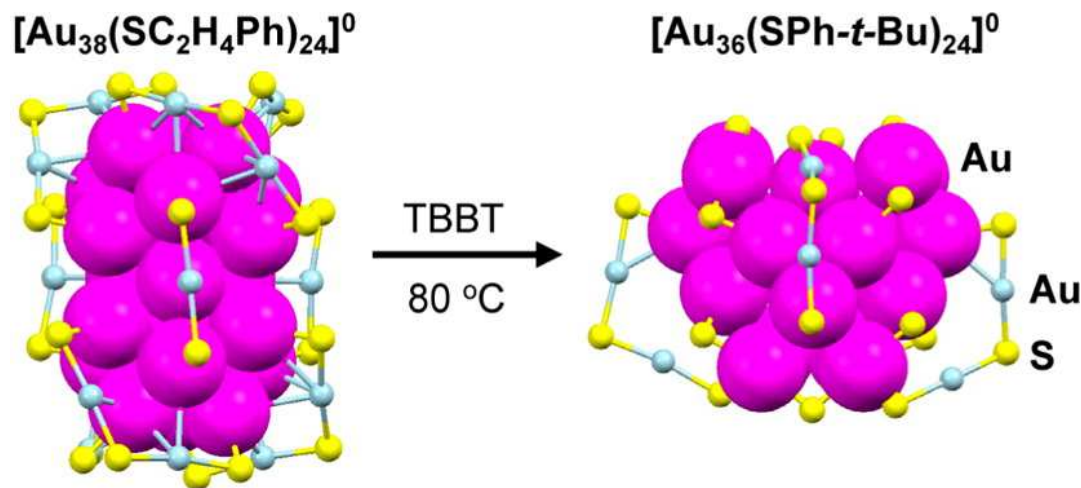


Thiol Ligand-Induced Transformation of $\text{Au}_{38}(\text{SC}_2\text{H}_4\text{Ph})_{24}$ to $\text{Au}_{36}(\text{SPh-t-Bu})_{24}$

Chenjie Zeng, Chunyan Liu, Yong Pei, and Rongchao Jin*

ACS NANO, Article ASAP



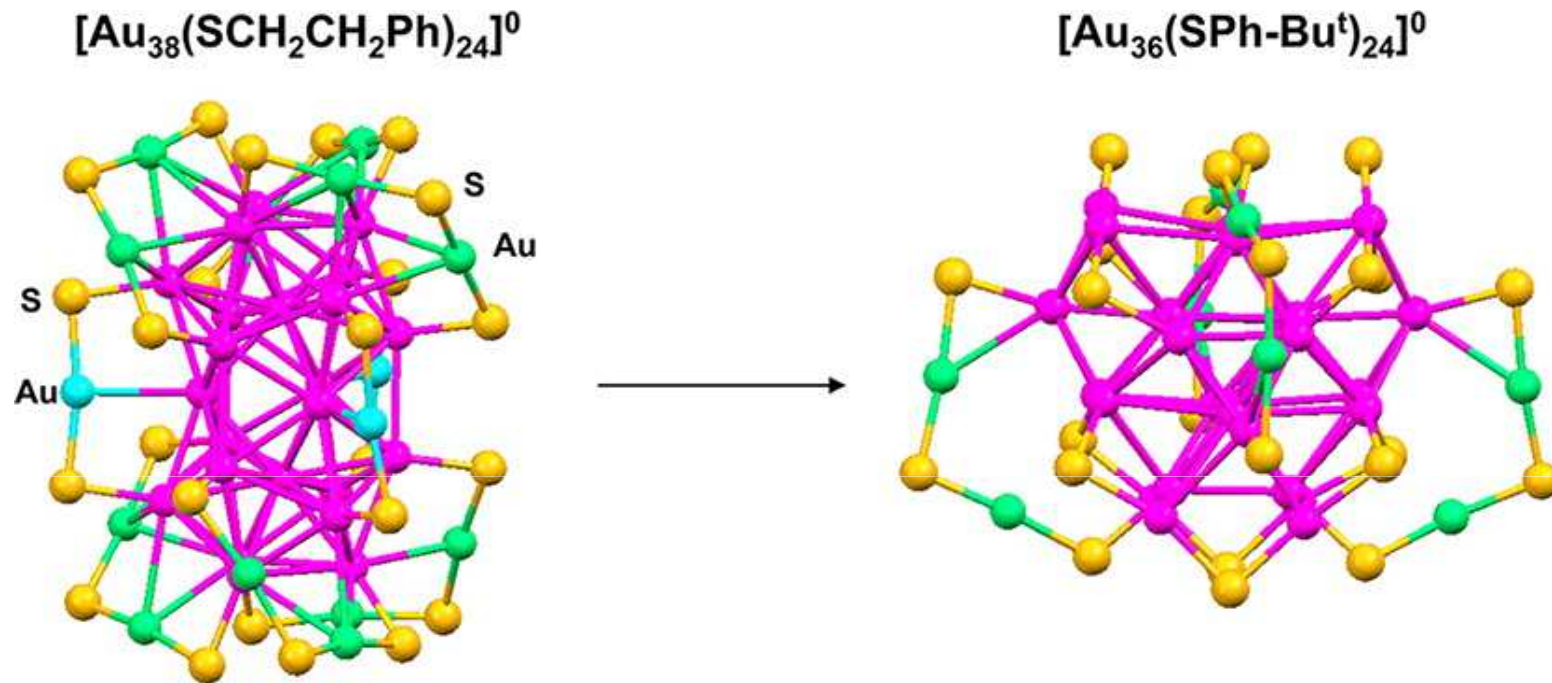
SHRIDEVI S BHAT
05/07/2013

INTRODUCTION

- The synthesis of thiolate-protected gold nanoclusters and studies of their properties have achieved significant advances in recent years.
- Size-focusing methodology has been successfully established giving rise to molecularly pure $\text{Au}_{25}(\text{SR})_{18}$, $\text{Au}_{38}(\text{SR})_{24}$, and $\text{Au}_{144}(\text{SR})_{60}$ nanoclusters and bimetal ones as well as some larger nanoclusters.
- In addition to the size-focusing method, another useful approach pertains to ligand exchange, such as phosphine-to-thiol exchange processes.
- However, in many cases molecular purity product could not be obtained except in the case of phosphine-capped Au_{11} to thiolate-capped Au_{25} .

IN THIS PAPER

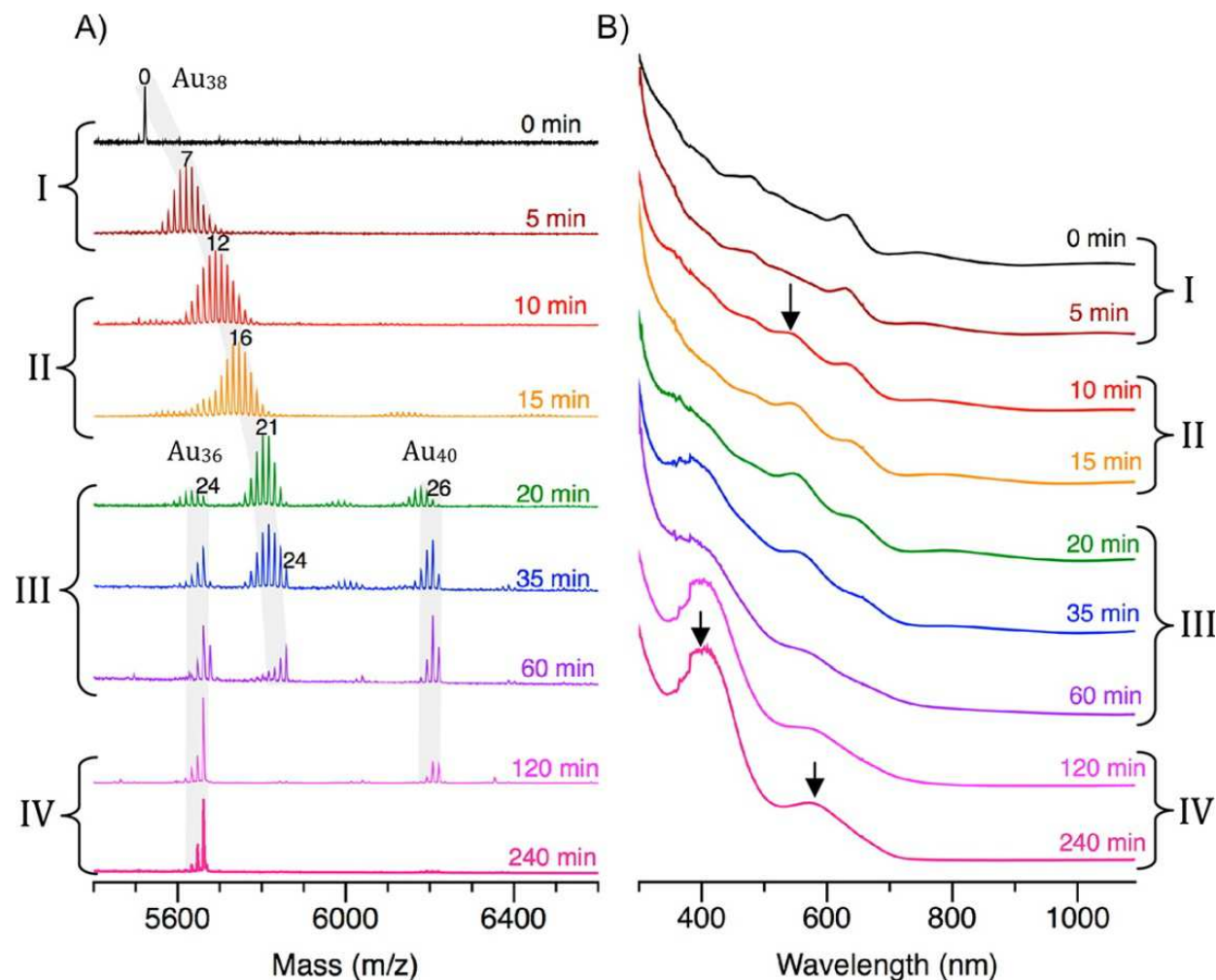
- An interesting disproportionation mechanism identified in the transformation of $\text{Au}_{38}(\text{PET})_{24}$ to $\text{Au}_{36}(\text{TBBT})_{24}$ is discussed.
- The ligand exchange reaction of $\text{Au}_{38}(\text{PET})_{24}$ with bulkier TBBT induces structural distortion of the initial rod-like biicosahedral $\text{Au}_{38}(\text{PET})_{24}$ structure.
- This process is evidenced by detailed mass spectrometric and optical spectroscopic analyses.
- The optical spectrum of $\text{Au}_{36}(\text{TBBT})_{24}$ was further interpreted by theoretical simulations on a $\text{Au}_{36}(\text{SCH}_3)_{24}$ model cluster.



Scheme 1: Conversion of $\text{Au}_{38}(\text{PET})_{24}$ to $\text{Au}_{36}(\text{TBBT})_{24}$ nanoclusters (the carbon tails are not shown for clarity; S atoms, yellow; kernel Au atoms, magenta; surface Au atoms, green or cyan).

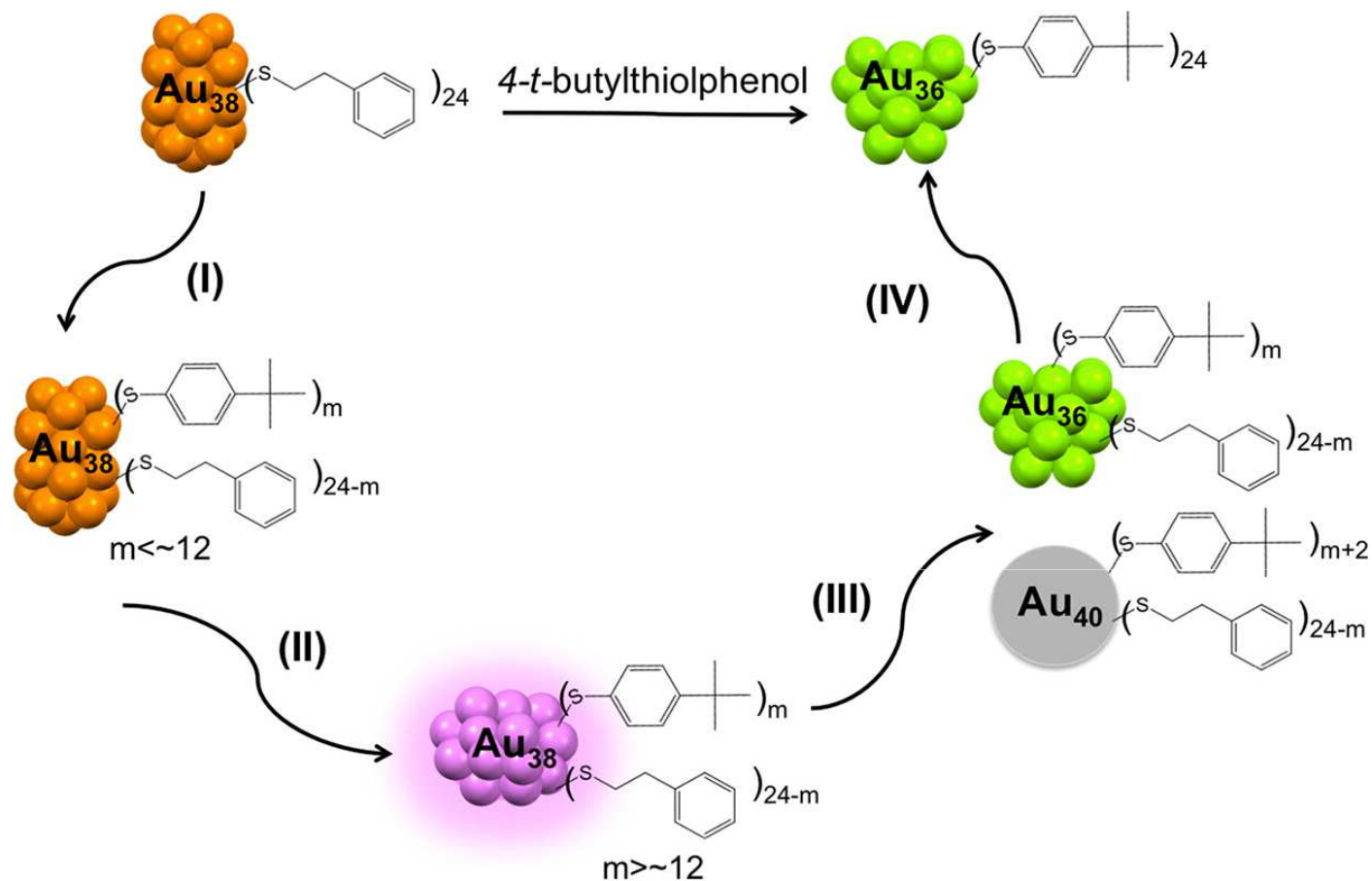
RESULTS AND DISCUSSION

- **Stage I:** In the first stage (0-5 min), ligand exchange reaction occurs.
- **Stage II:** In this stage (10-15 min), the ligand exchange reaction continues, but it starts to induce structural distortion of the original $\text{Au}_{38}(\text{SR})_{24}$ cluster, as manifested in the optical spectra.
- **Stage III:** It is in this critical stage (20-60 min) that the size and structural conversions take place.
- **Stage IV:** During the fourth stage (120-300 min), during which a size focusing conversion occurs together with further ligand exchange toward completion.



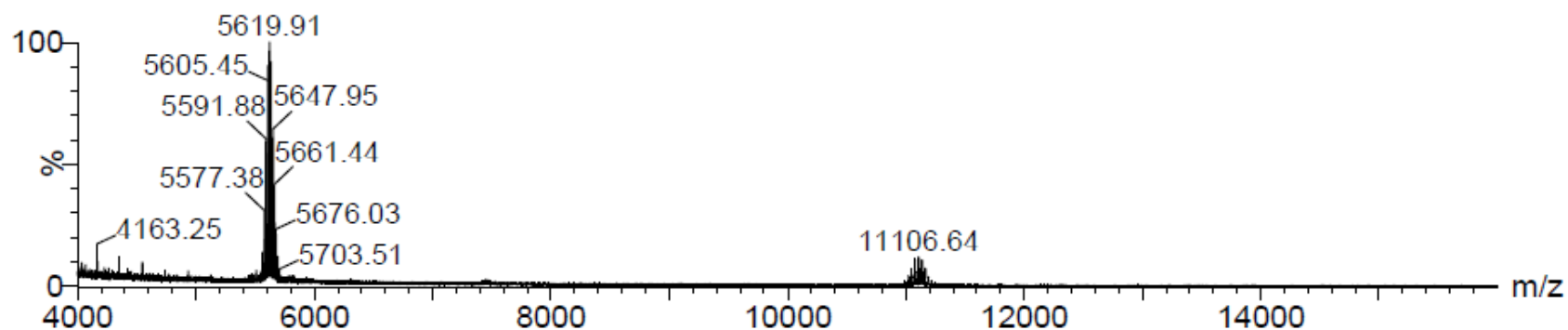
(A) Time-dependent ESI-MS of the transformation reaction. The doubly charged region is shown. The three gray shadows indicate three groups of peaks: (left) $Au_{36}(TBBT)_m(PET)_{24-m}$, (middle) $Au_{38}(TBBT)_m(PET)_{24-m}$, (right) $Au_{40}(TBBT)_{m+2}(PET)_{24-m}$. The numbers on the top of the mass peaks indicate the number of TBBT ligands (m) exchanged onto the cluster.

(B) Corresponding UV-vis spectra of different times in parallel with ESI-MS.

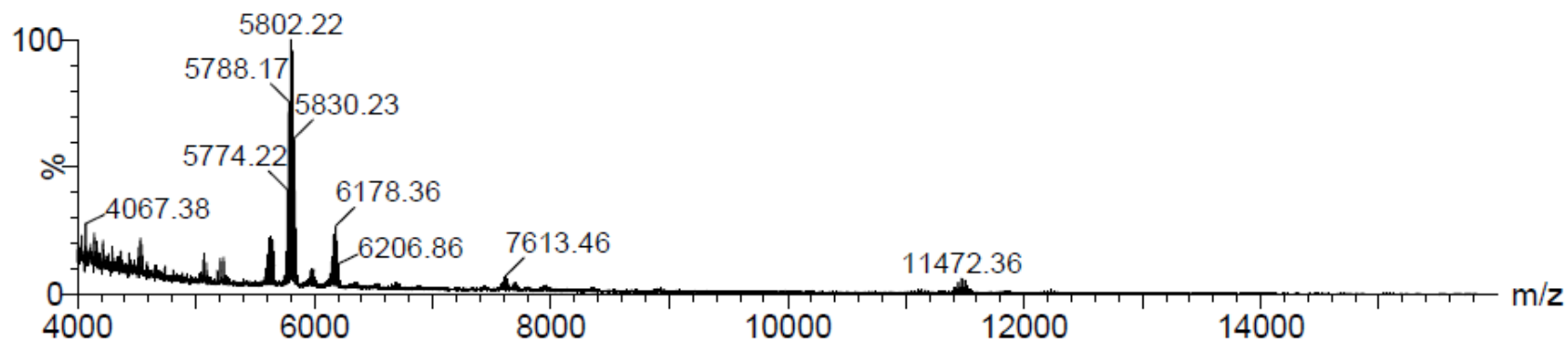


Scheme 2: Reaction pathway for conversion of $\text{Au}_{38}(\text{PET})_{24}$ to $\text{Au}_{36}(\text{TBBT})_{24}$. Stage I, ligand exchange; II, structure distortion; III, disproportionation; IV, size focusing.

A) Full range ESI-MS spectrum for the 5-min product:



B) Full range ESI-MS spectrum for the 20-min product:



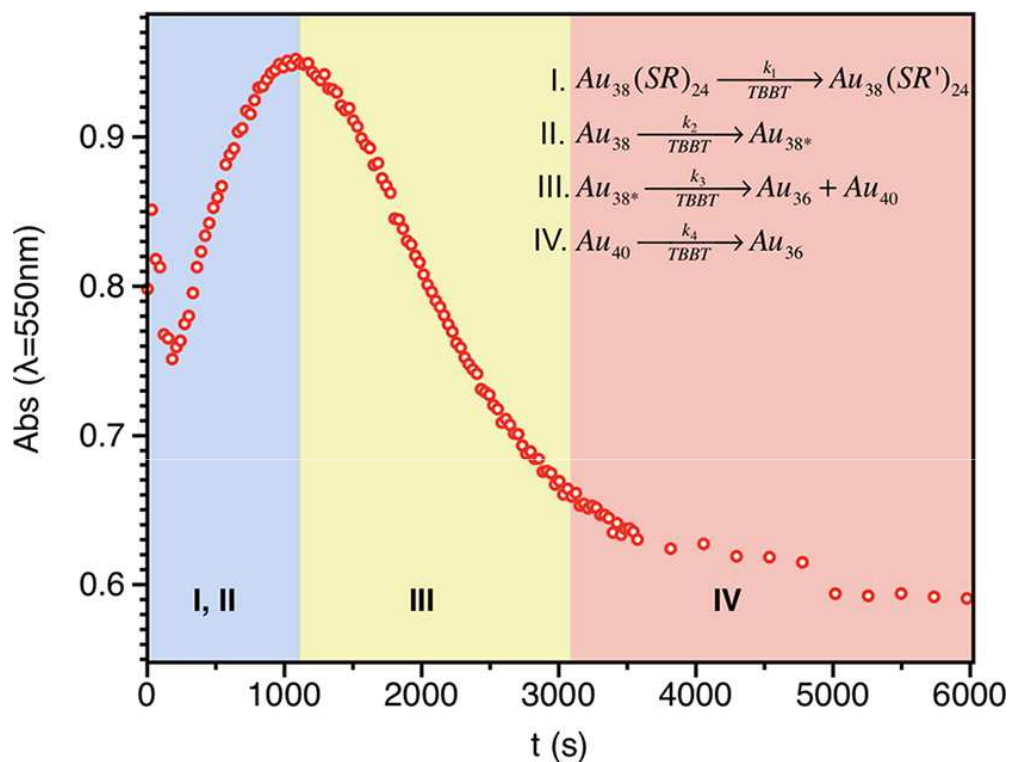


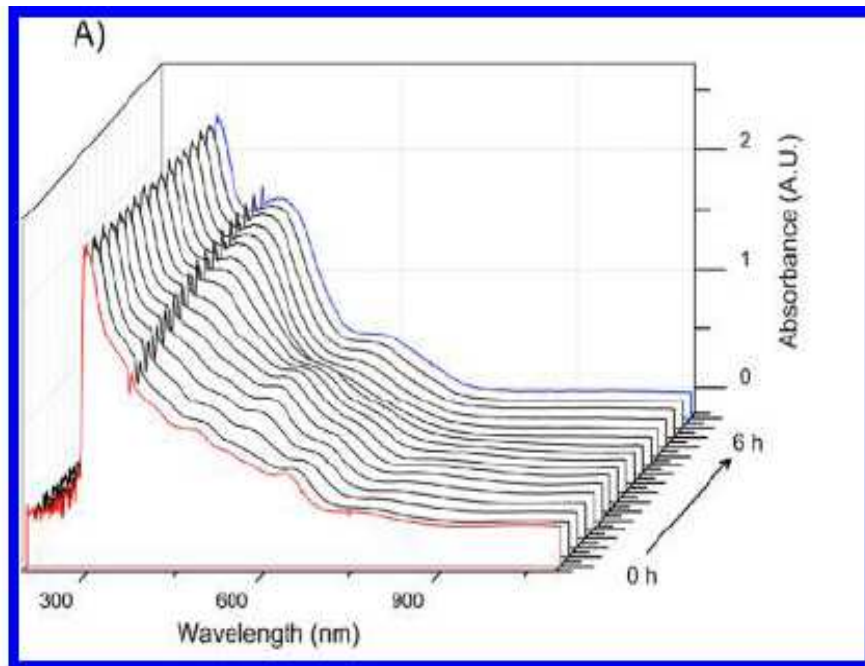
TABLE 1. Rate Constants for Stages II and III at Different Reaction Temperatures

	60 °C	70 °C	80 °C
$k_{2,obs} (s^{-1})$	4.0×10^{-4}	1.4×10^{-3}	3.5×10^{-3}
$k_{3,obs} (s^{-1})$	4.8×10^{-5}	1.8×10^{-4}	1.1×10^{-3}

$$E_{a,II} = 107 \text{ kJ/mol}$$

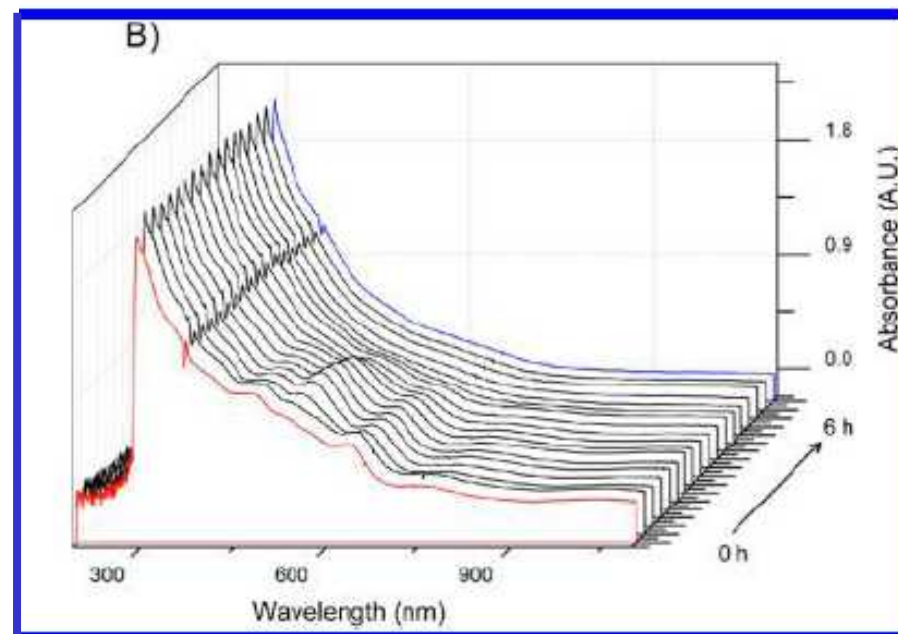
$$E_{a,III} = 152 \text{ kJ/mol}$$

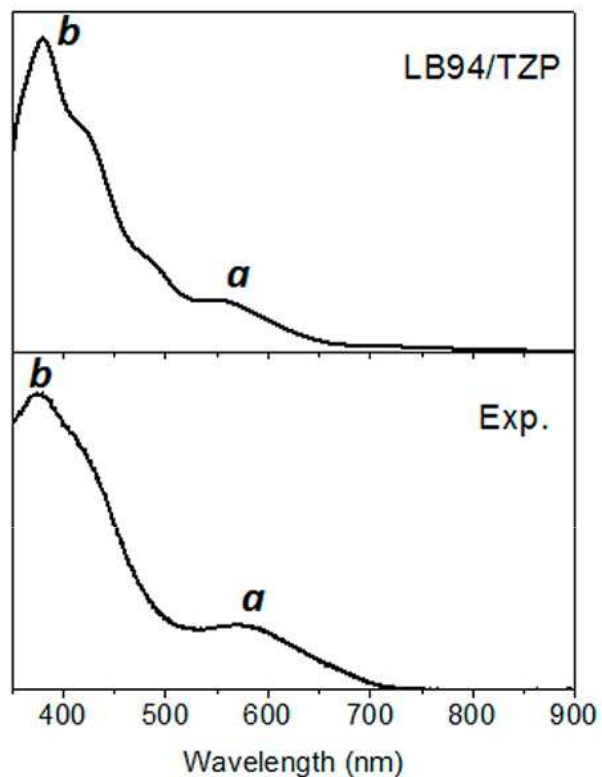
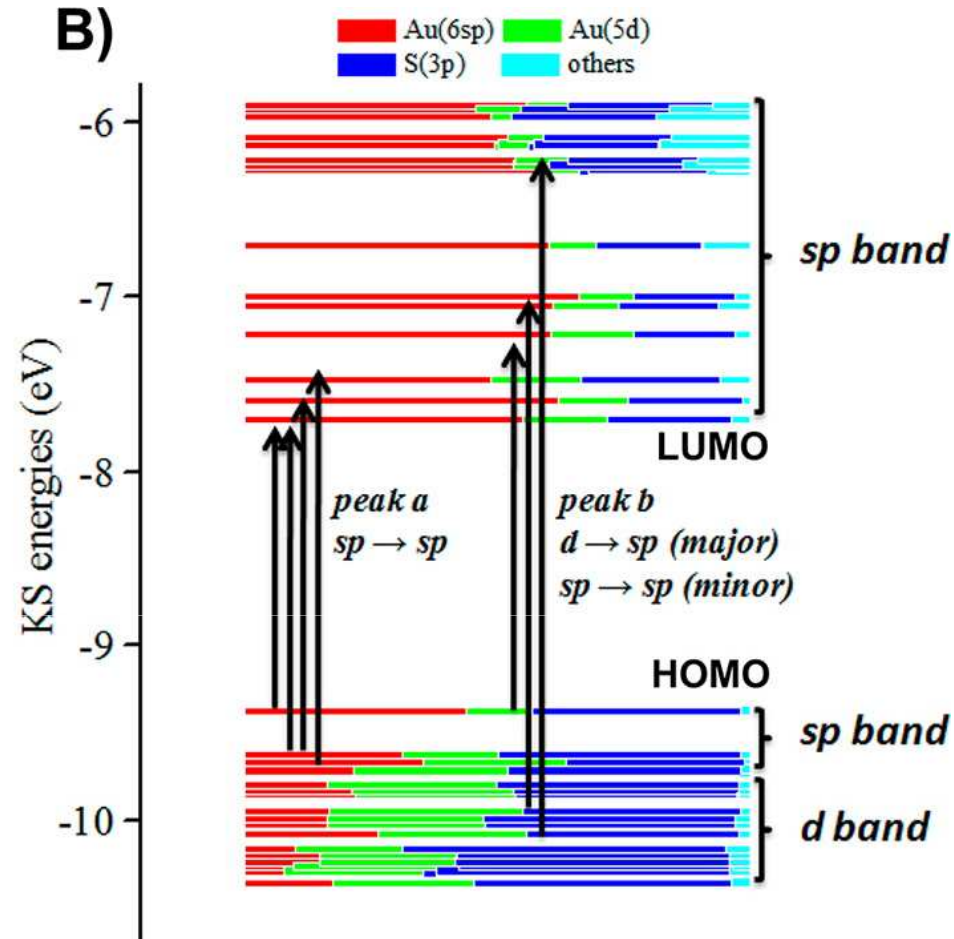
Kinetic curve (monitored by absorbance at 550 nm) for the conversion of $Au_{38}(PET)_{24}$ to $Au_{36}(TBBT)_{24}$ at 80 ° C.



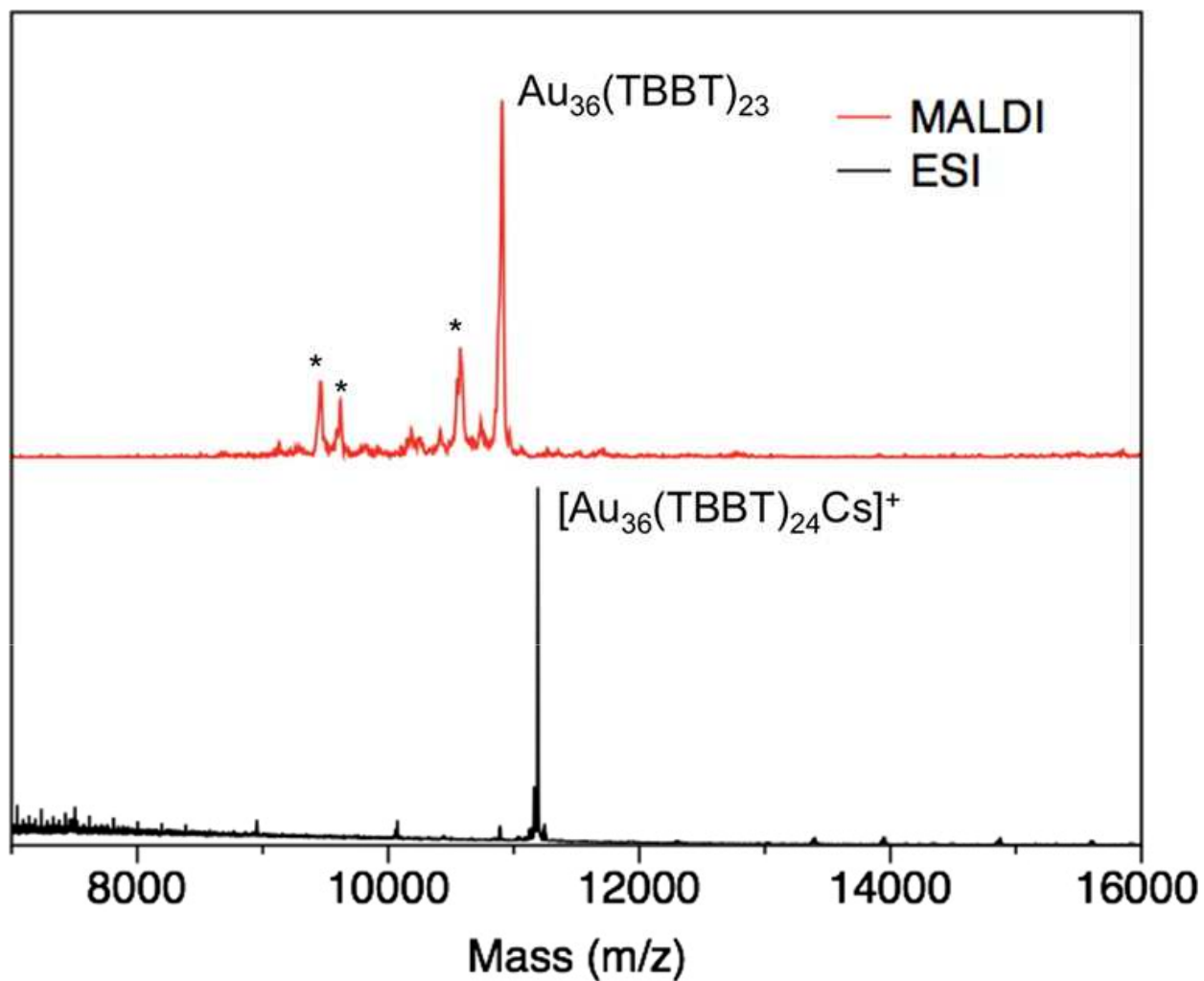
Time-dependent UV-vis spectral evolution of 4-*tert*-butylbenzenethiol with $\text{Au}_{38}(\text{PET})_{24}$.

Time-dependent UV-vis spectral evolution of cyclohexanethiol reaction with $\text{Au}_{38}(\text{PET})_{24}$.



A)**B)**

(A) Comparison of simulated UV-vis absorption spectrum of $\text{Au}_{36}(\text{SR})_{24}$ with the experimental spectrum. (B) Estimation of contributions of Au(6sp), Au(5d), and S(3p) to KS orbitals.



Comparison of the MALDI-MS and ESI-MS spectra of $\text{Au}_{36}(\text{TBBT})_{24}$. The asterisks indicate the fragments due to MALDI.

CONCLUSION

- The detailed mechanism of the ligand-induced conversion from $\text{Au}_{38}(\text{PET})_{24}$ to $\text{Au}_{36}(\text{TBBT})_{24}$ is discussed.
- The reaction pathway can be roughly divided into four stages.
- This process gave rise to Au_{36} nanoclusters in $\sim 90\%$ yield (Au atom basis), approaching the theoretical yield of $\sim 94\%$ according to the disproportionation mechanism.
- The conversion of biicosahedral Au_{38} structure to fcc Au_{36} structure is remarkable; it provides an unprecedented example of ligand bulkiness induced size and structural transformation in thiolate-protected nanoclusters.

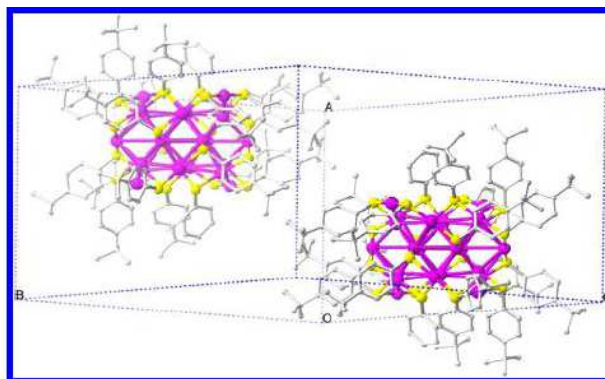
SIGNIFICANCE

The role of ligand in the formation and crystallization of clusters!

Chiral Structure of Thiolate-Protected 28-Gold-Atom Nanocluster
Determined by X-ray Crystallography

Chenjie Zeng, Tao Li, Anindita Das, Nathaniel L. Rosi, and Rongchao Jin*.

J|A|C|S
JOURNAL OF THE AMERICAN CHEMICAL SOCIETY





THANK YOU